Characterization of position sensitive detectors with positioning algorithms trained by simulated reference data

V.Y. Pedash

Institute for scintillation materials NAS of Ukraine

Kharkov, Ukraine

Introduction: Parallax error in PET

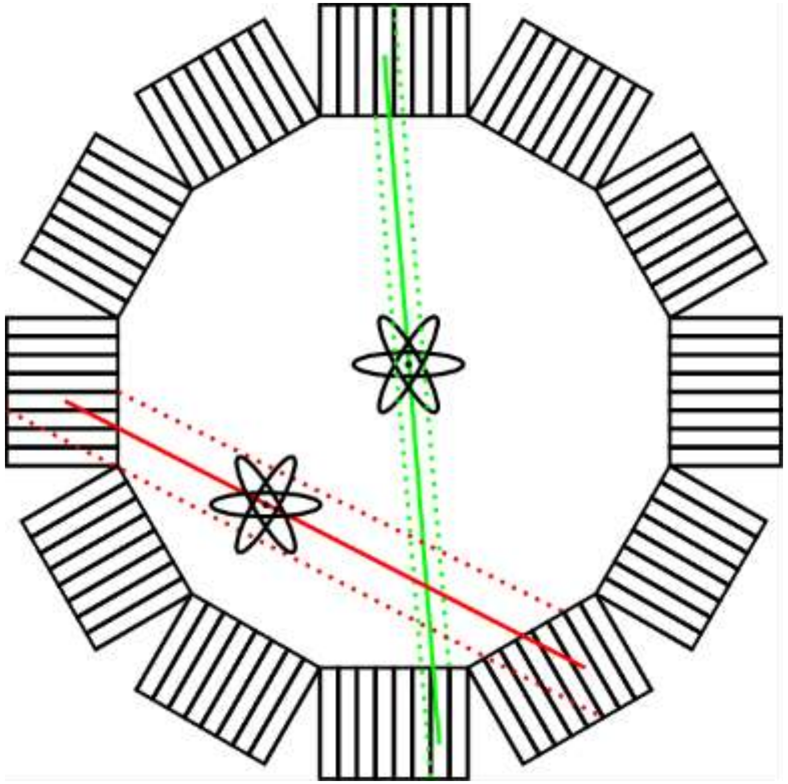

- Degrades spatial resolution at the edges of field-of-view (FOV)
- More important for small FOV dedicated scanners and preclinical imagers
- Can be mitigated by 3D reconstruction of point-of-interaction (POI)

Introduction: 3D POI reconstruction

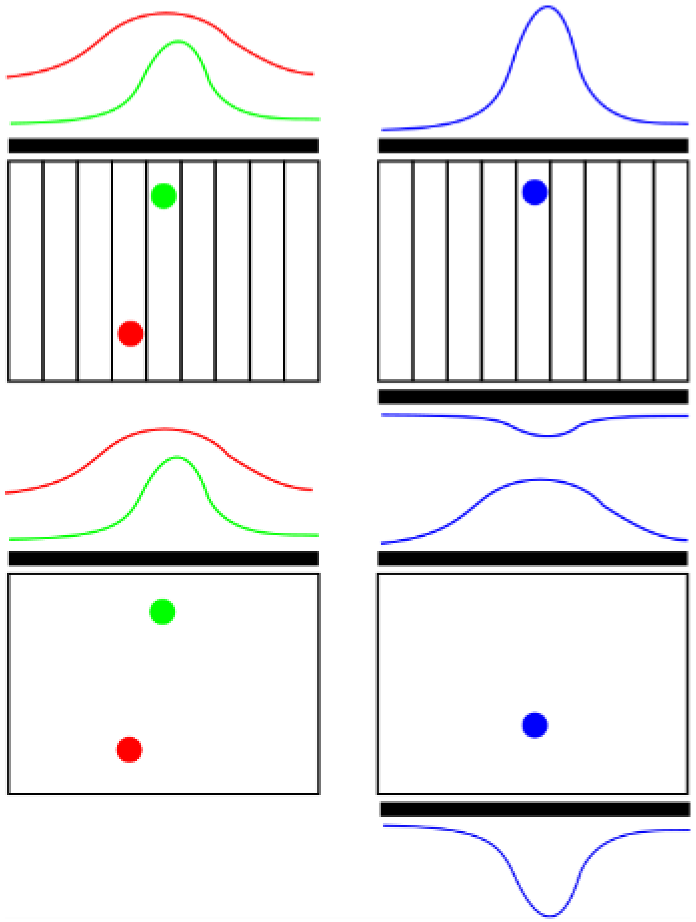

- Single and dual side readout of homogeneous and pixilated crystals
- Light distribution over position sensitive photodetector depends on POI position
- Controlled crosstalk between pixels

Introduction: Reconstruction algorithms

- Analytical

$$X_c = \frac{\sum_j \left(\sum_i n_{i,j}\right)^{\alpha} x_j}{\sum_j \left(\sum_i n_{i,j}\right)^{\alpha}}$$

IEEE TRANSACTIONS ON NUCLEAR SCIENCE

A Novel Method for γ-photons Depth-of-Interaction Detection in Monolithic Scintillation Crystals

Roberto Pani, *Member, IEEE*, Marco Bettiol, Enrico Preziosi, Cristian Borrazzo, Rosanna Pellegrini, Antonio J. González, Pablo Conde, Maria Nerina Cinti, Andrea Fabbri, Elisabetta Di Castro, and Stan Majewski

- Machine learning

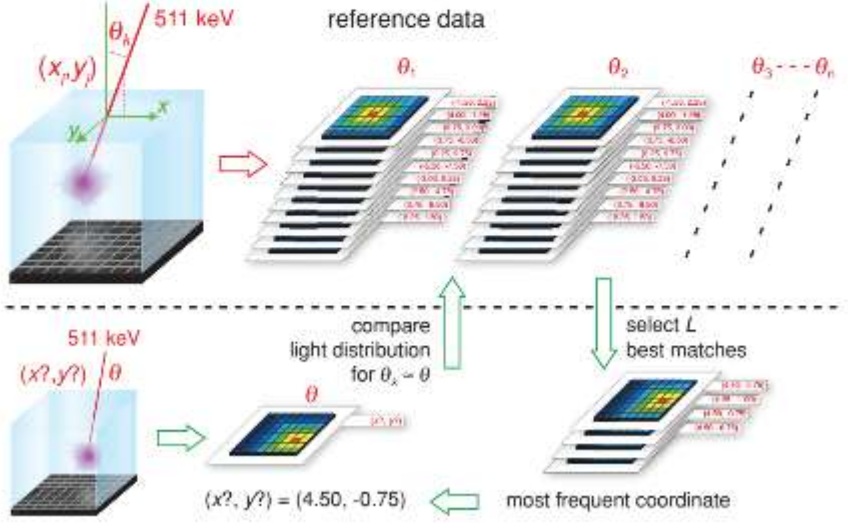

IOP Publishing Physics in Medicine and Biology
Phys. Med. Biol. 54 (2009) 3501–3512 doi:10.1088/0031-9155/54/11/015

A novel, SiPM-array-based, monolithic scintillator detector for PET

Dennis R Schaart[1], Herman T van Dam[1], Stefan Seifert[1], Ruud Vinke[2], Peter Dendooven[2], Herbert Löhner[2] and Freek J Beekman[1,3]

Introduction: Typical calibration procedure

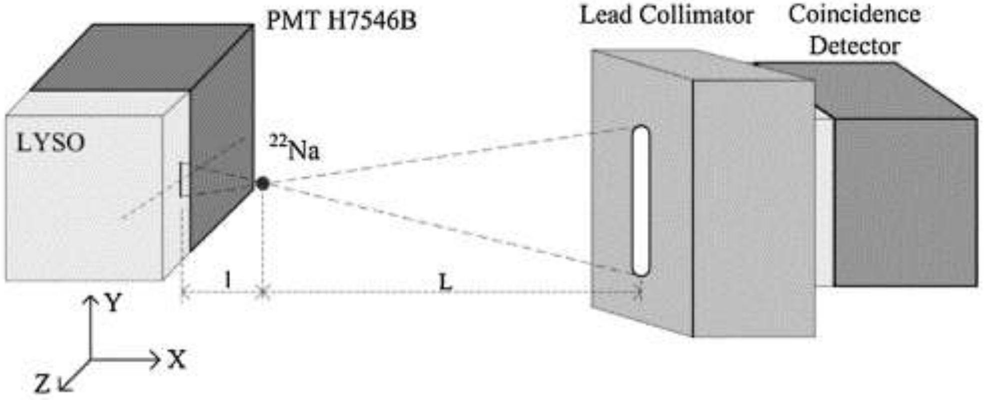

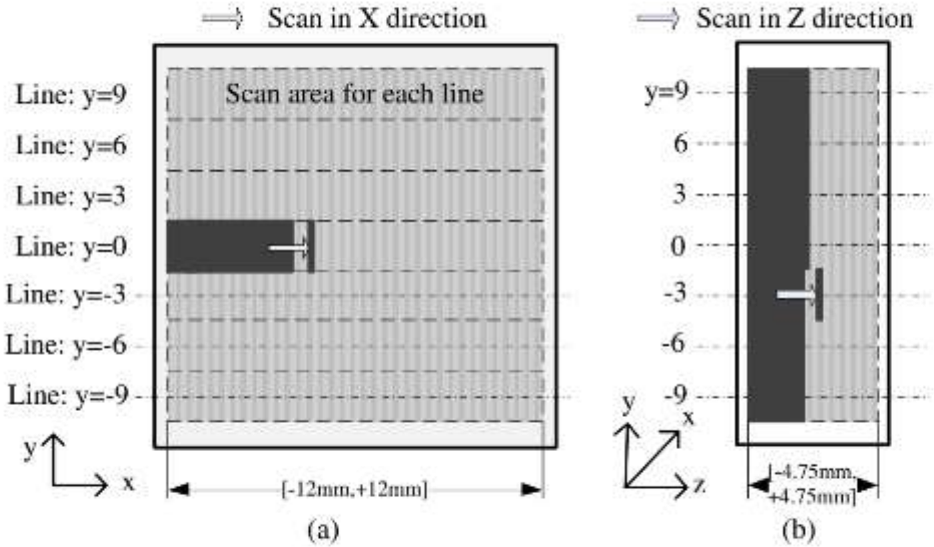

IOP Publishing — Physics in Medicine and Biology

Phys. Med. Biol. **58** (2013) 1375–1390 — doi:10.1088/0031-9155/58/5/1375

3D position estimation using an artificial neural network for a continuous scintillator PET detector

Y Wang, W Zhu, X Cheng and D Li

Main objectives

- Using Monte-Carlo simulation study the influence of scattering distance in the gaps on the performance of pixilated detectors
- Build and test a positioning algorithm for 3D position sensitive detectors using reference data obtained from GEANT4 simulations
- Characterize detectors based on pixilated and homogeneous crystals using estimators from previous step

Simulation: detector design

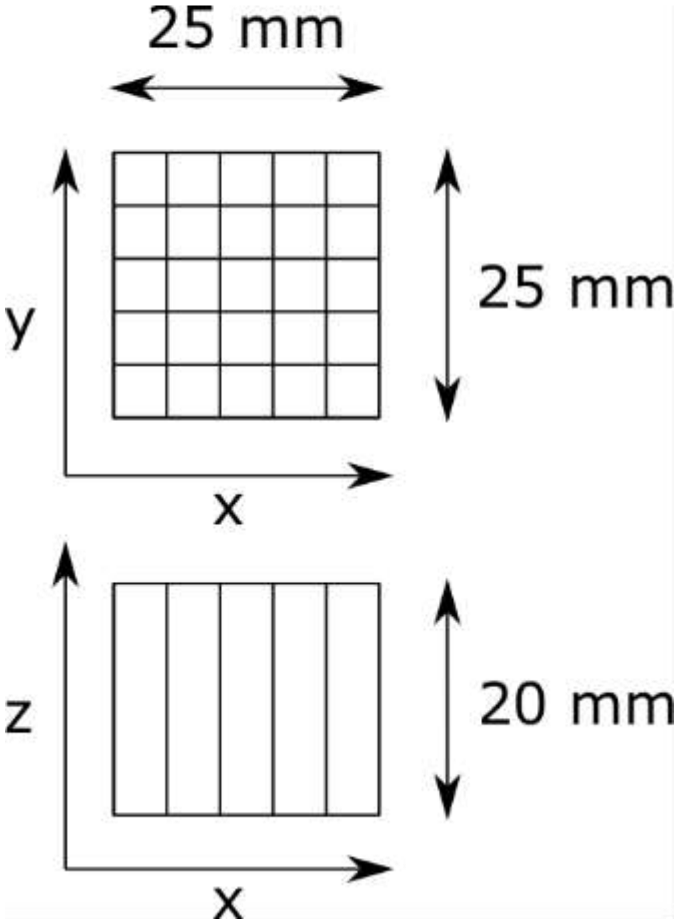

- Single side readout
- Pixel size 4.75 x 4.75 x 20 mm^3
- 0.5 mm inter pixel gap
- Pixilated crystal (PC) with transparent optical contact between pixels
- Homogeneous crystal (HC) with laser induced optical barriers formed by sub-surface laser engraving
- Outer surface covered by diffusive reflector (DR) or black absorber (BA)
- LYSO:Ce

Simulation: setup

Model

- 20000 events
- 10000 photons per event
- 70% for training and 30% for verification
- 10 iterations for each estimator
- Select the best estimator based on MAE for X and Z axis

Estimators

- Neural network: 2 hidden layers with 25 neurons in each one
- Neuron activation functions: logistic, ReLU, tanh
- K-nearest neighbors : k = 5, Manhattan distance

Simulation: Influence of scattering distance in septa on light spread function

- Homogeneous crystal and diffusive reflector (HC DR). Z = 10 mm

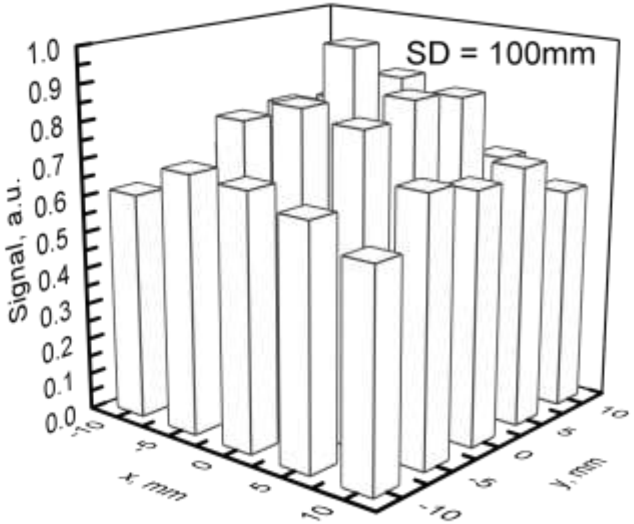

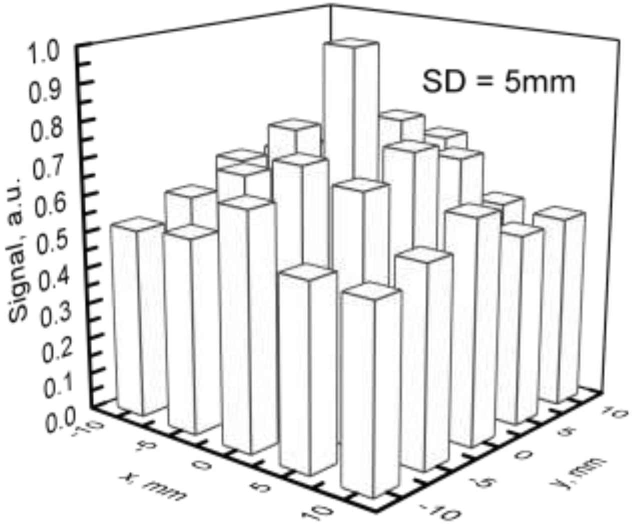

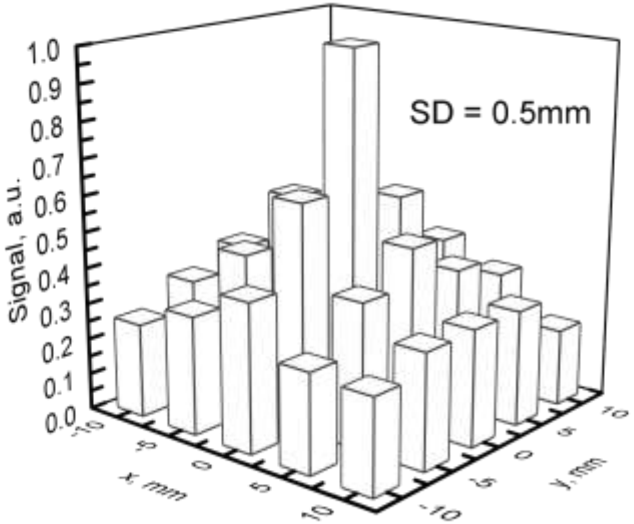

Simulation: Influence of DOI position on light spread function

- Pixilated crystal and diffusive reflector (PC DR). SD = 100 mm

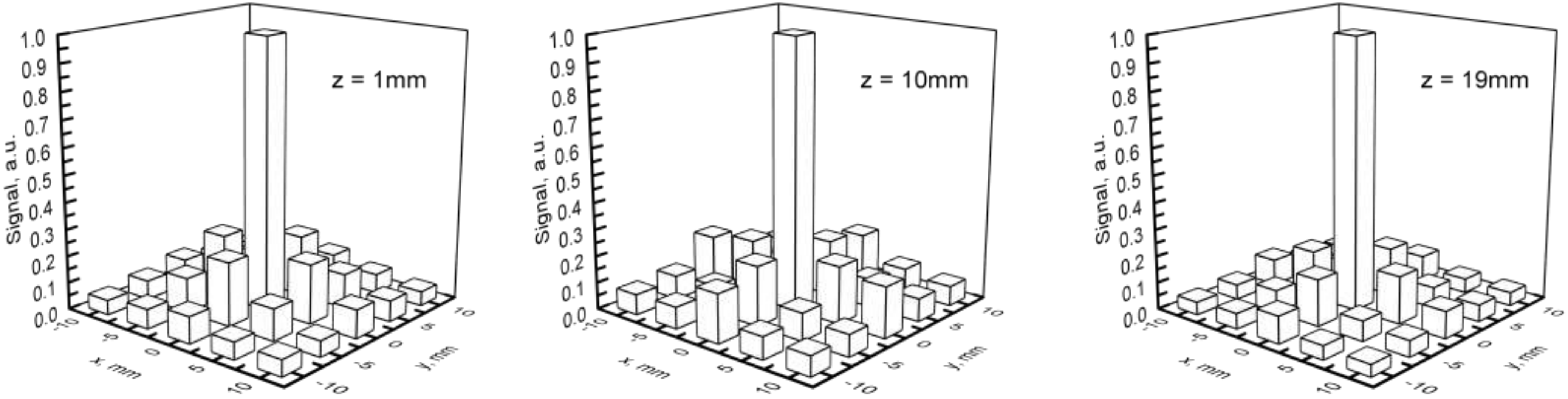

Simulation: Homogeneous crystal and diffusive reflector (HC DR)

Scattering distanse	X RMSE, mm	X MAE, mm	X, Learning algorithm	Z RMSE, mm	Z MAE, mm	Z, Learning algorithm
0.1	1.092	0.899	Neural network (tanh)	0.654	0.413	Neural network (tanh)
0.3	0.805	0.624	Neural network (tanh)	0.614	0.392	Neural network (tanh)
0.5	0.79	0.608	Neural network (tanh)	0.677	0.444	Neural network (tanh)
0.7	0.796	0.607	Neural network (tanh)	0.73	0.471	Neural network (tanh)
1	0.846	0.649	Neural network (tanh)	0.872	0.56	Neural network (ReLu)
3	0.87	0.657	Neural network (tanh)	1.343	0.902	Neural network (tanh)
5	0.867	0.647	Neural network (tanh)	1.461	0.935	Neural network (ReLu)
10	0.878	0.639	Neural network (tanh)	1.439	0.983	Neural network (tanh)
20	0.901	0.632	Neural network (tanh)	1.374	0.939	Neural network (tanh)
100	0.93	0.632	Neural network (ReLu)	1.316	0.903	Neural network (ReLu)

Simulation: Homogeneous crystal and black absorber (HC BA)

Scattering distanse	X RMSE, mm	X MAE, mm	X, Learning algorithm	Z RMSE, mm	Z MAE, mm	Z, Learning algorithm
0.1	1.162	0.938	kNN	0.681	0.403	kNN
0.3	0.795	0.625	Neural network (tanh)	0.692	0.421	kNN
0.5	0.702	0.545	Neural network (tanh)	0.683	0.44	kNN
0.7	0.685	0.526	Neural network (tanh)	0.721	0.454	kNN
1	0.664	0.509	Neural network (tanh)	0.812	0.517	kNN
3	0.703	0.526	Neural network (tanh)	1.172	0.769	kNN
5	0.703	0.518	Neural network (tanh)	0.916	0.653	Neural network (tanh)
10	0.671	0.481	Neural network (tanh)	0.706	0.497	Neural network (ReLu)
20	0.591	0.419	Neural network (tanh)	0.619	0.453	Neural network (tanh)
100	0.493	0.353	Neural network (tanh)	0.537	0.4	Neural network (tanh)

Simulation: Pixilated crystal and diffusive reflector (PC DR)

Scattering distanse	X RMSE, mm	X MAE, mm	X, Learning algorithm	Z RMSE, mm	Z MAE, mm	Z, Learning algorithm
0.1	1.124	0.874	kNN	1.206	0.553	kNN
0.3	1.095	0.851	kNN	1.365	0.979	Neural network (tanh)
0.5	1.081	0.842	kNN	1.465	1.057	Neural network (tanh)
0.7	1.068	0.829	kNN	1.606	1.122	Neural network (tanh)
1	1.046	0.805	kNN	1.799	1.218	Neural network (tanh)
3	0.964	0.735	kNN	2.828	1.275	kNN
5	0.953	0.724	kNN	2.699	1.22	kNN
10	0.937	0.711	kNN	2.536	1.12	kNN
20	0.899	0.681	kNN	2.456	1.058	kNN
100	0.886	0.668	kNN	2.237	0.974	kNN

Simulation: Pixilated crystal and black absorber (PC BA)

Scattering distanse	X RMSE, mm	X MAE, mm	X, Learning algorithm	Z RMSE, mm	Z MAE, mm	Z, Learning algorithm
0.1	1.094	0.842	kNN	1.204	0.544	kNN
0.3	1.081	0.84	kNN	1.49	0.739	kNN
0.5	1.053	0.814	kNN	1.62	0.795	kNN
0.7	1.038	0.794	kNN	1.322	0.965	Neural network (tanh)
1	1.002	0.768	kNN	1.471	1.008	Neural network (tanh)
3	0.928	0.7	kNN	2.51	1.08	kNN
5	0.915	0.678	kNN	2.092	0.924	kNN
10	0.875	0.656	kNN	1.576	0.751	kNN
20	0.853	0.633	kNN	1.308	0.678	kNN
100	0.848	0.632	kNN	1.109	0.621	kNN

Simulation: Positioning along X axis

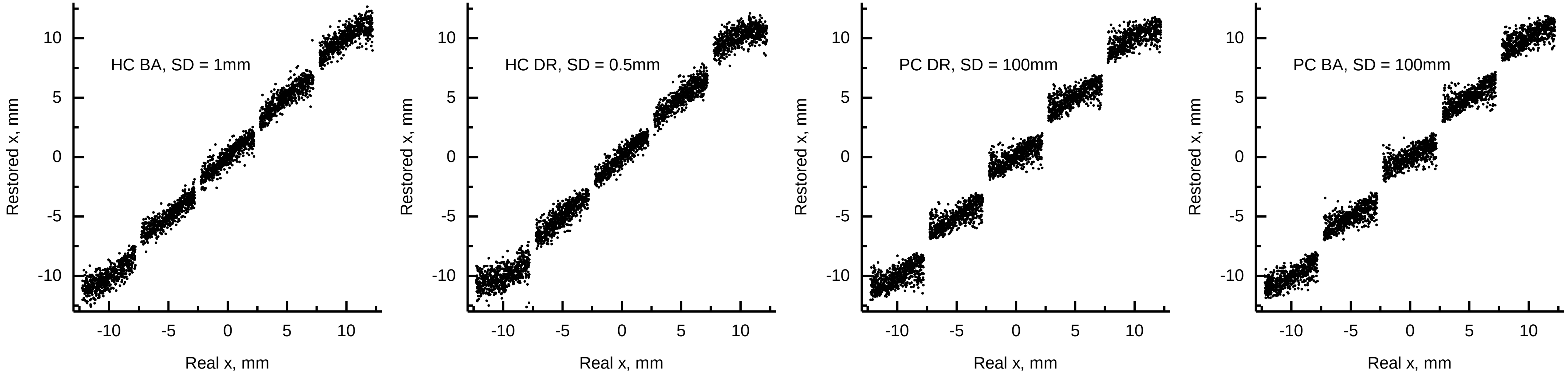

Simulation: Positioning along Z axis

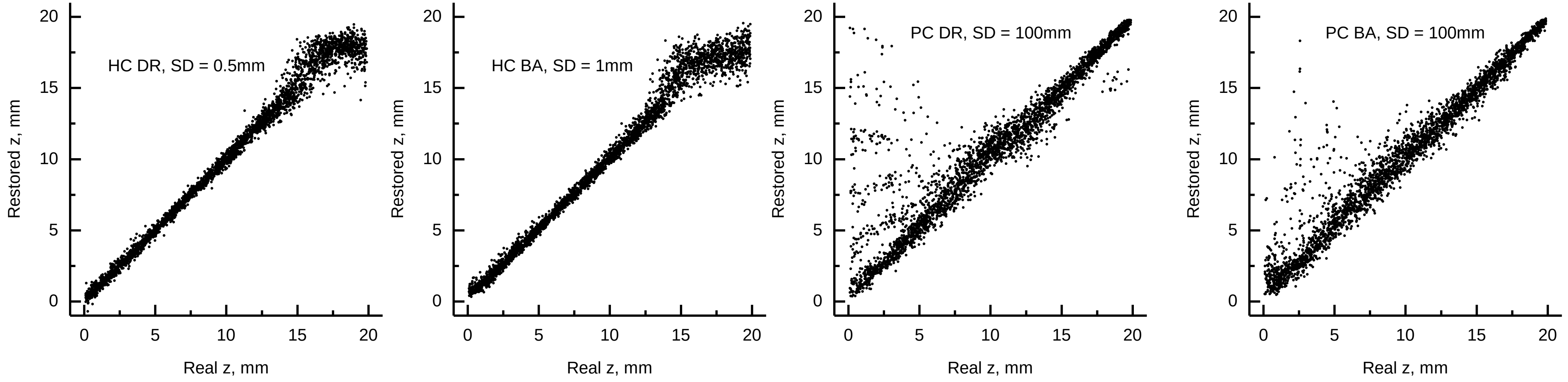

Simulation: Spatial resolution

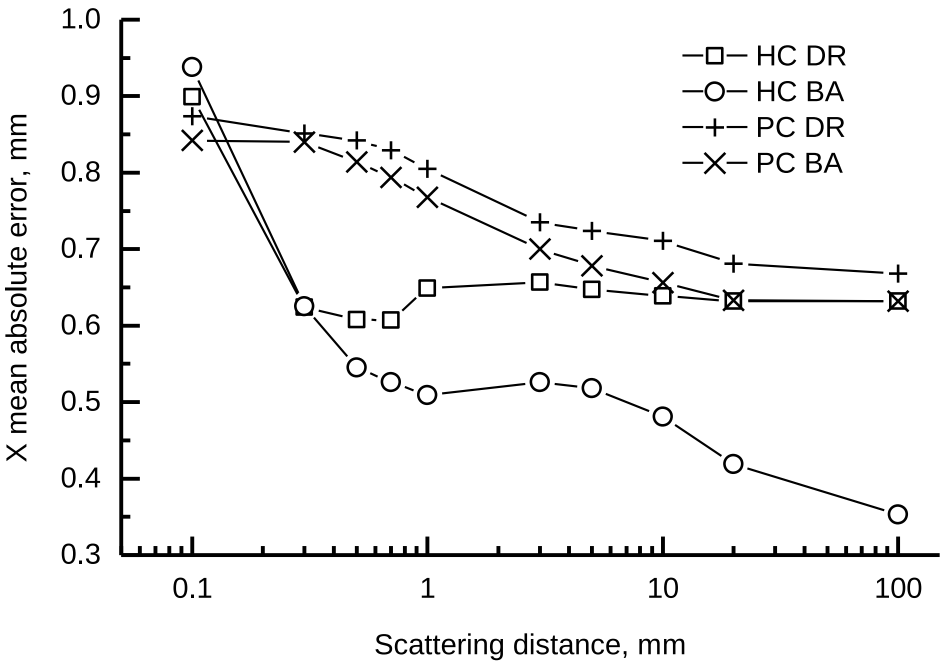

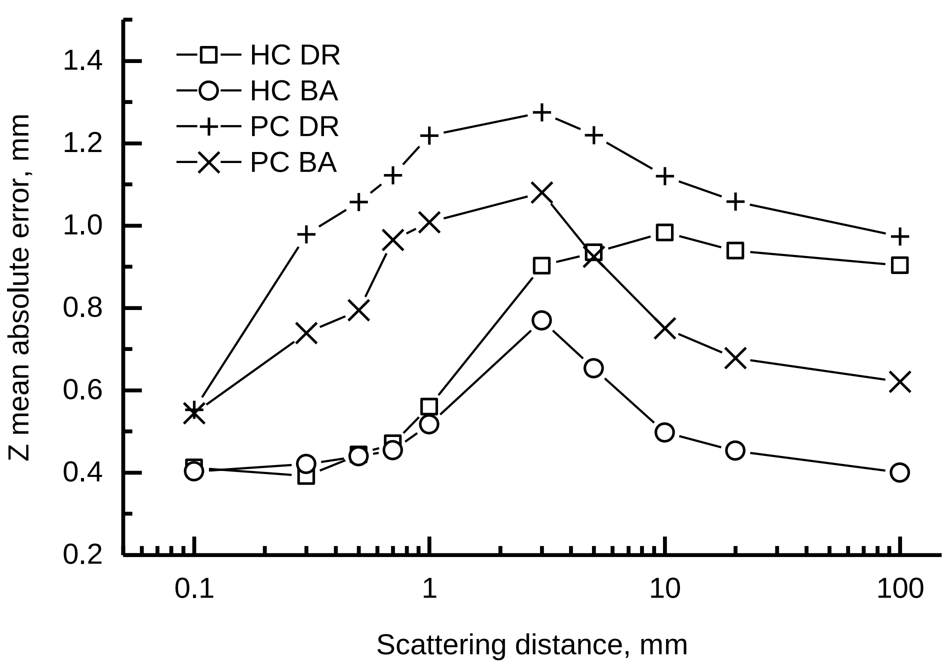

Simulation: Light collection

Light collection

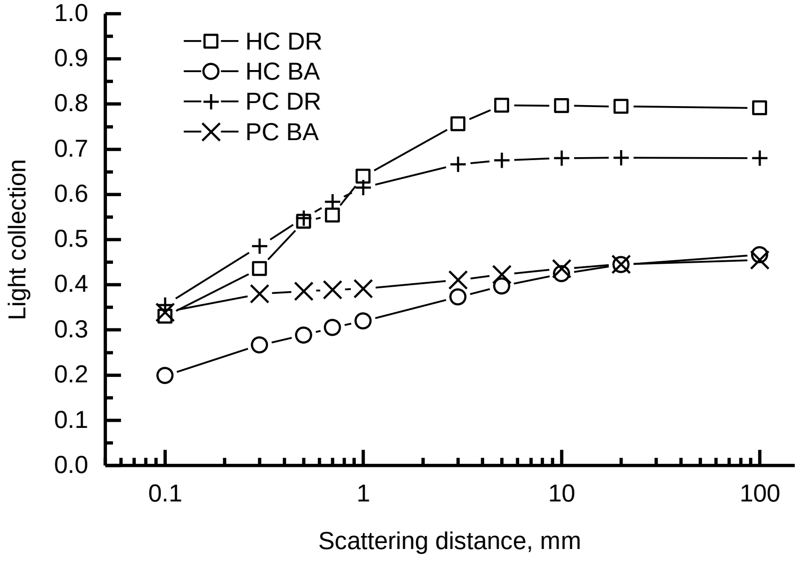

Light collection uniformity

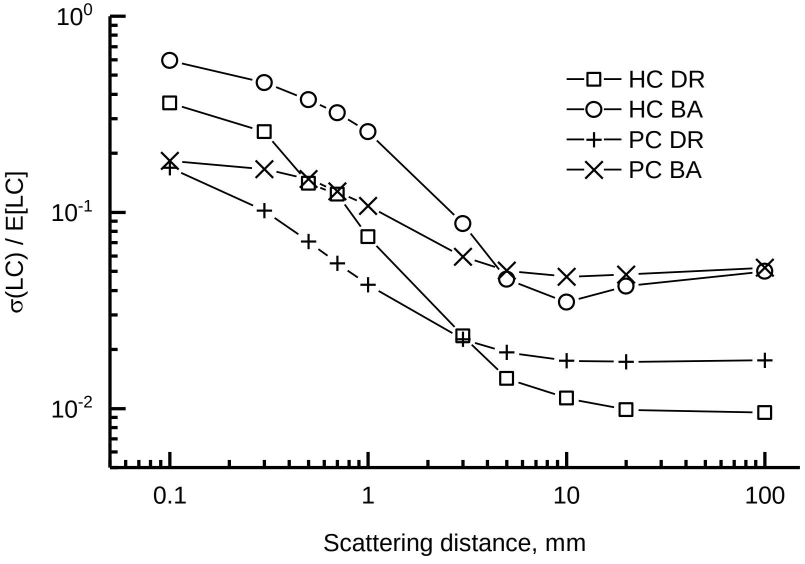

Experiment: detector design

Homogeneous crystal

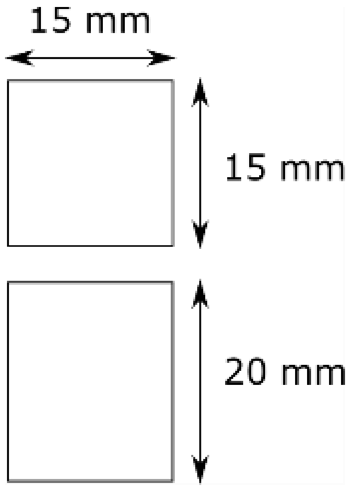

- CsI:Tl
- All surfaces polished

Pixilated crystal

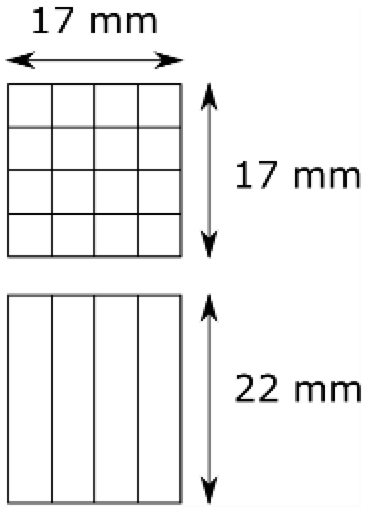

- LYSO:Ce
- Pixel size: 4x4x22 mm^3
- All surfaces polished
- No perfect pixel match to SiPM dies

Experiment: DAQ

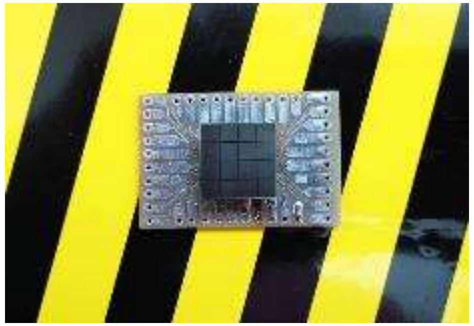

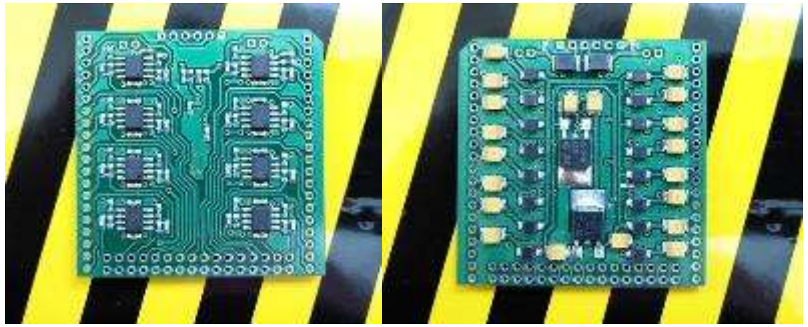

- Hamamatsu S13361 SiPM
- 16 (4×4) ch
- 3x3 mm^2 photosensitive area
- 3584 pixels
- 50x50 μm^2 pixel size

- 16 ch preamplifier
- Gain = 30

- 8 ch DAQ
- 12 bit ADC
- 40 MHz sampling rate
- Ethernet interface

Experiment: Setup

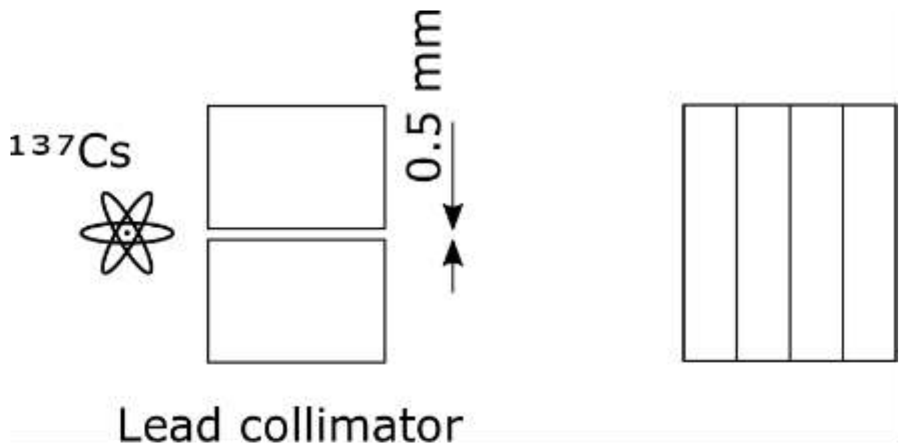

- Energy and spatial resolution was measured using 662 keV gamma photons from ^{137}Cs source

Results: Energy resolution

PC DR

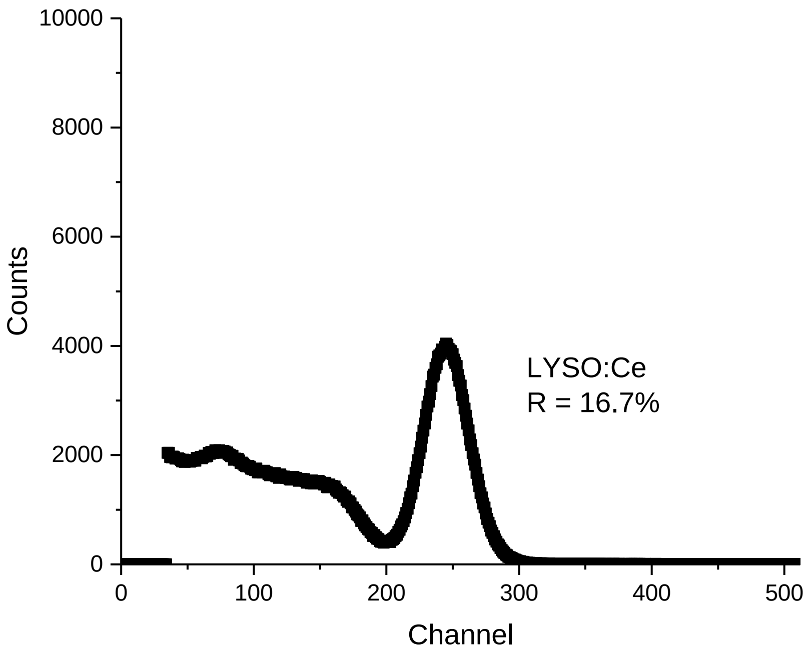

HC DR

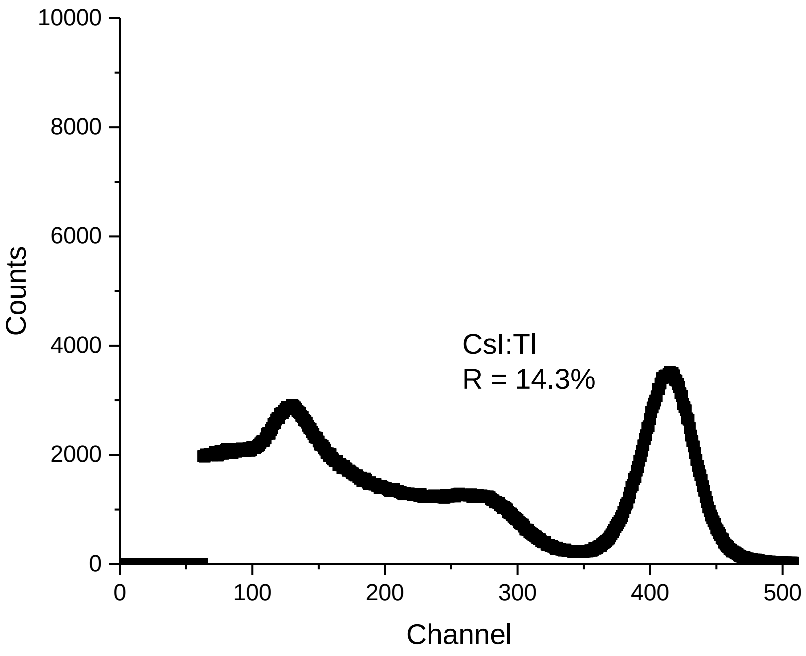

Results: 3D reconstruction

HC DR

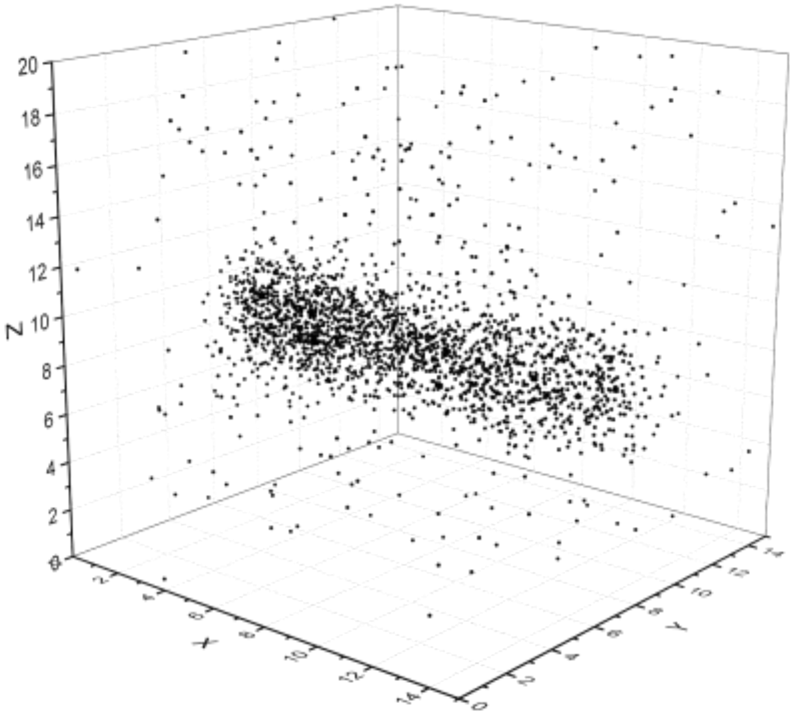

PC DR

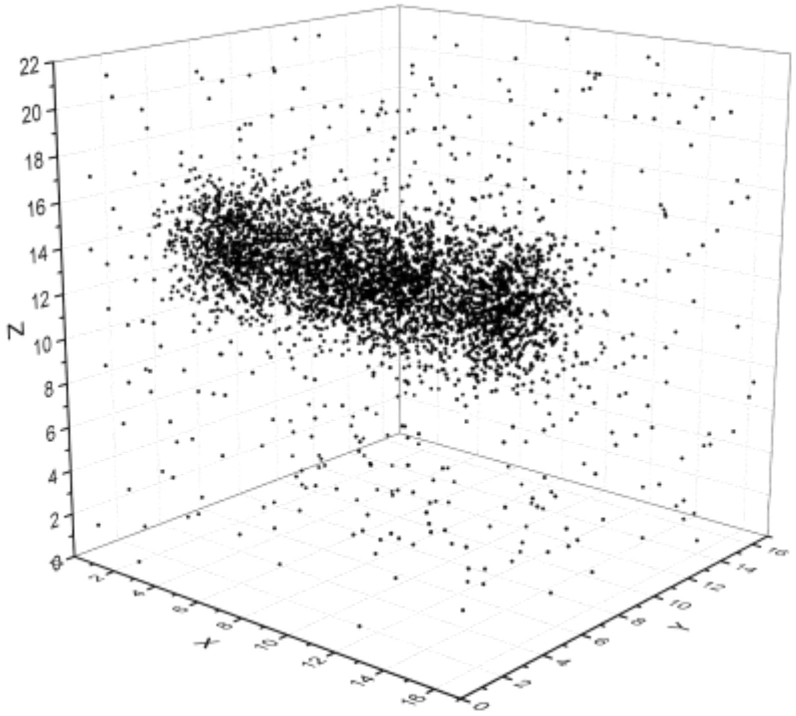

Results: Spatial resolution - HC DR

#	Y, mm	Z, mm	σ Y, mm	σ Z, mm
1	7.6	8.3	1.1	1.5
2	7.3	3.1	0.9	1.1
3	11.7	17.3	1.2	1.7
4	6.2	17.1	1	1.8

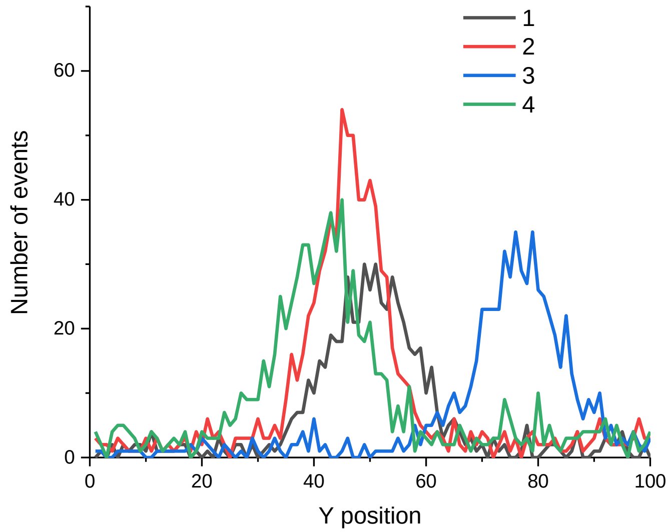

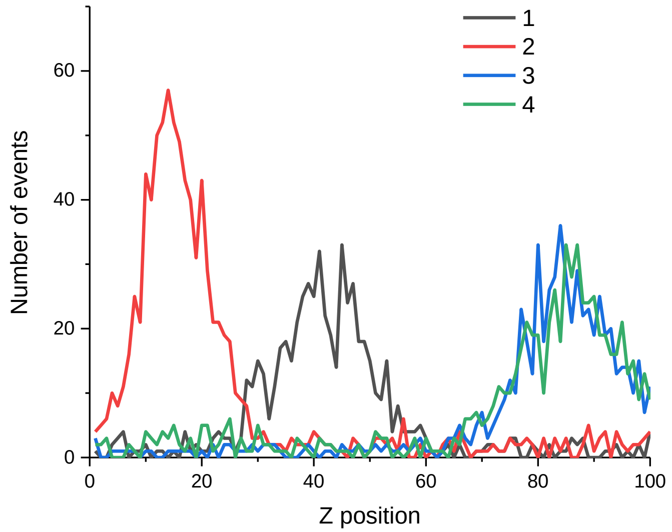

Results: Spatial resolution - PC DR

#	Y, mm	Z, mm	σ Y, mm	σ Z, mm
1	5.8	13.2	1.4	1.2
2	6.1	3.4	1.7	0.9
3	14.3	18.6	2.2	1.3
4	6.4	19.1	2.0	1.3

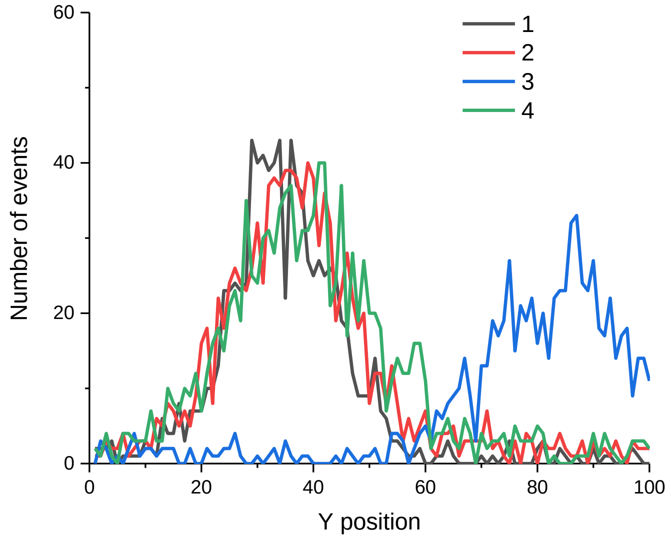

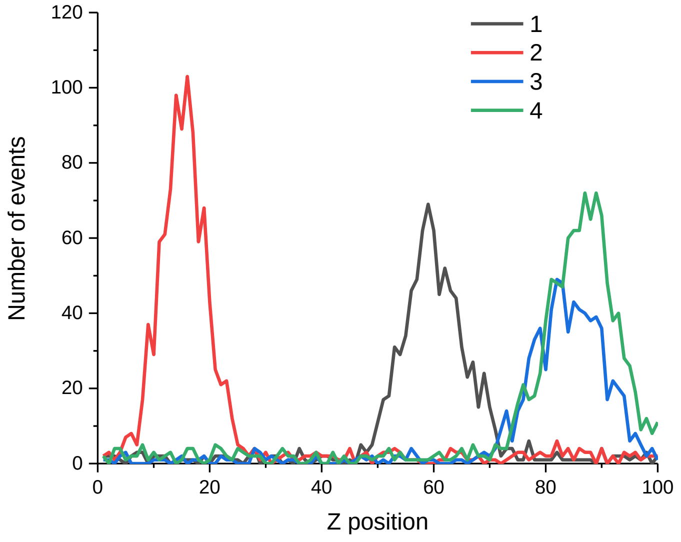

Conclusions

- Introduction of laser induced optical barriers into monolithic crystal wrapped into black absorber doesn't improve accuracy of positioning light collection and light collection uniformity
- Laser induced optical barriers with scattering distance bigger then the septa width in monolithic crystal wrapped into diffusive reflector improves DOI reconstruction in the detector and minimally affect positioning in XY plane as well as light collection and light collection uniformity
- According to simulation the best performance in pixilated detectors can be achieved when gaps between pixels are filled with transparent optical contact
- Simulated reference data can be effectively used to train positioning algorithms for 3D position sensitive detectors for PET
- There is a possibility to achieve sub-pixel resolution in both detectors based on pixilated crystal and monolithic one treated by sub-surface laser engravement